AGU PUBLICATIONS

Geophysical Research Letters

RESEARCH LETTER
10.1002/2013GL058315

Key Points:
- Sea ice loss (2.6 W m−2) and clouds (1.2 W m−2) explain RCP8.5 absorbed SW changes
- Southern Ocean radiatively important clouds (RIC) are low-level liquid clouds
- RIC respond primarily to warming and stability changes, not poleward jet shifts

Supporting Information:
- Readme
- Figure S1
- Figure S2

Correspondence to:
J. E. Kay,
jenkay@ucar.edu

Citation:
Kay, J. E., B. Medeiros, Y.-T. Hwang, A. Gettelman, J. Perket, and M. G. Flanner (2014), Processes controlling Southern Ocean shortwave climate feedbacks in CESM, *Geophys. Res. Lett.*, *41*, 616–622, doi:10.1002/2013GL058315.

Received 14 OCT 2013
Accepted 9 DEC 2013
Accepted article online 11 DEC 2013
Published online 21 JAN 2014

Processes controlling Southern Ocean shortwave climate feedbacks in CESM

J. E. Kay[1,2], B. Medeiros[1], Y.-T. Hwang[3], A. Gettelman[1], J. Perket[4], and M. G. Flanner[4]

[1]Climate and Global Dynamics Division, National Center for Atmospheric Research, Boulder, Colorado, USA, [2]Now at Department of Atmospheric and Oceanic Sciences, University of Colorado, Boulder, Colorado, USA, [3]Scripps Institution of Oceanography, University of California, San Diego, La Jolla, California, USA, [4]Department of Atmospheric, Oceanic, and Space Sciences, University of Michigan, Ann Arbor, Michigan, USA

Abstract A climate model (Community Earth System Model with the Community Atmosphere Model version 5 (CESM-CAM5)) is used to identify processes controlling Southern Ocean (30–70°S) absorbed shortwave radiation (ASR). In response to 21st century Representative Concentration Pathway 8.5 forcing, both sea ice loss (2.6 W m^{-2}) and cloud changes (1.2 W m^{-2}) enhance ASR, but their relative importance depends on location and season. Poleward of ~55°S, surface albedo reductions and increased cloud liquid water content (LWC) have competing effects on ASR changes. Equatorward of ~55°S, decreased LWC enhances ASR. The 21st century cloud LWC changes result from warming and near-surface stability changes but appear unrelated to a small (1°) poleward shift in the eddy-driven jet. In fact, the 21st century ASR changes are 5 times greater than ASR changes resulting from large (5°) naturally occurring jet latitude variability. More broadly, these results suggest that thermodynamics (warming and near-surface stability), not poleward jet shifts, control 21st century Southern Ocean shortwave climate feedbacks.

1. Motivation

Recent Southern Ocean studies have examined observed cloud processes and cloud/sea ice influence on radiative fluxes [e.g., *Haynes et al.*, 2011; *Fitzpatrick and Warren*, 2007], quantified and ameliorated climate model cloud biases [e.g., *Williams et al.*, 2013; *Bodas-Salcedo et al.*, 2013], and correlated Southern Ocean shortwave biases and feedbacks to global circulation biases [e.g., *Hwang and Frierson*, 2013; *Ceppi et al.*, 2012] and to climate sensitivity [e.g., *Trenberth and Fasullo*, 2010]. In contrast, understanding the physical processes underlying Southern Ocean climate feedbacks has received less attention.

Modeled Southern Ocean cloud-climate feedbacks vary greatly in their sign and magnitude. A transition from positive shortwave cloud feedbacks in the subtropics to negative shortwave cloud feedbacks near the Antarctic continent is seen in the multimodel mean [*Vial et al.*, 2013, Figure 8; *Zelinka et al.*, 2013, Figure 8f]. This intermodel spatial pattern consistency suggests that similar processes control Southern Ocean cloud-climate feedbacks in many models. *Tsushima et al.* [2006] found that extratropical cloud phase changes including a "poleward shift of cloud water" over the Southern Ocean were important but did not assess the influence of other potentially important processes such as poleward jet/storm track shifts [*Yin*, 2005; *Barnes and Polvani*, 2013] or Antarctic sea ice loss [*Lefebvre and Goosse*, 2008].

Motivated to improve our physical understanding of Southern Ocean climate feedbacks, we identify and evaluate processes controlling modeled Southern Ocean absorbed shortwave radiation (ASR) changes in response to 21st century forcing and natural jet variability. The processes controlling ASR also control shortwave feedbacks (typically estimated as ASR change normalized by surface warming).

2. Model Simulations

We use a coupled climate model, the Community Earth System Model with the Community Atmosphere Model version 5 (CESM-CAM5) [*Hurrell et al.*, 2013], at 1° horizontal resolution. We analyze four transient 21st century simulations forced by historical and Representative Concentration Pathway 8.5 (RCP8.5) forcing [*Meinshausen et al.*, 2011; *Lamarque et al.*, 2011] and 1000 years of a stable and balanced control simulation with constant preindustrial (1850 Common Era) forcing. Over the 21st century (2080–2099 minus 2006–2025), CESM-CAM5 global mean (Southern Ocean (30–70°S)) surface temperatures increase by 3.5 K (2.9 K). Unlike the late twentieth century

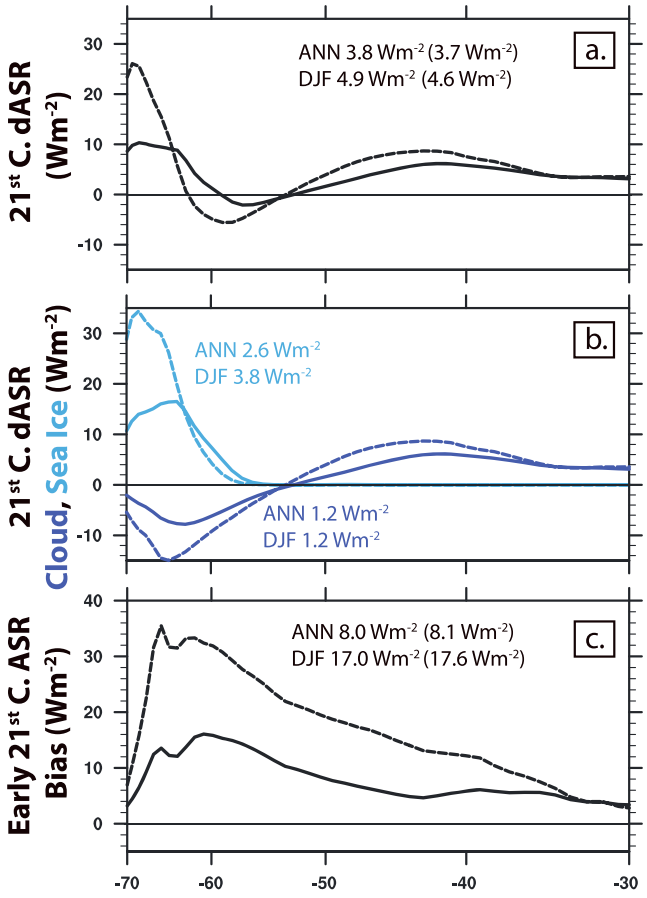

Figure 1. Zonal mean CESM-CAM5 absorbed shortwave radiation (ASR): (a) RCP8.5 21st century top-of-model ASR change (dASR, 2080–2099 minus 2007–2026), (b) RCP8.5 21st century top-of-model dASR due to cryospheric changes (change in cryospheric radiative effect (dCrRE)) and cloud changes (dASR-dCrRE), (c) early 21st century top-of-atmosphere ASR bias (CESM-CAM5 minus CERES-EBAF v2.7 observations 2000–2012) [*Loeb et al.*, 2009]. Solid curves are annual means. Dashed curves are Southern Hemisphere summer (DJF) means. Plotted lines based on single-ensemble member (CrRE_RCP8.5_CAM5_CN_07), which had CrRE calculations. Mean Southern Ocean (30–70°S) values for this single ensemble and for the ensemble mean (in parentheses when available) are reported. For Figure 1c, the plotted bias uses model years 2007–2015, while the ensemble mean bias uses model years 2000–2012. These year selection differences had a small influence on the assessed ASR bias.

when the ozone hole had a dominant influence on Southern Hemisphere atmospheric circulation changes, the 2.5 times increase in equivalent CO_2 concentration over the 21st century in RCP8.5 overwhelms the influence of stratospheric ozone recovery [*Thompson et al.*, 2011].

3. Results

3.1. Southern Ocean ASR Changes and Biases

Over the 21st century, annual mean Southern Ocean (30–70°S) ASR increases by 3.8 Wm^{-2} under RCP8.5 forcing. The annual zonal mean ASR change vacillates in sign with latitude, exhibiting two peaks of enhanced ASR centered near 65°S and 42°S bracketing reduced ASR centered near 57°S (Figure 1a). These transient ASR changes have a similar sign and zonal mean shape as equilibrium Southern Ocean shortwave feedbacks in CAM5 [*Gettelman et al.*, 2012, Figure 5] and in the multimodel mean [*Vial et al.*, 2013; *Zelinka et al.*, 2013].

To separate the influence of sea ice and clouds on ASR changes, we used in-line cryospheric radiative effect (CrRE) [*Flanner et al.*, 2011] and residual cloud radiative effect (rCRE = ASR − CrRE) calculations at the top of the model. Sea ice loss (dCrRE = +2.6 W m^{-2}) is approximately twice as important as cloud changes (drCRE = +1.2 W m^{-2}) for explaining annual mean Southern Ocean ASR changes, but the influence of sea ice and clouds on ASR changes depends on latitude and on season (Figure 1b).

Sea ice loss explains enhanced ASR at the high Southern latitudes (~65°S peak in Figure 1a). Increased cloud reflection explains reduced ASR (~57°S trough in Figure 1a), while decreased cloud reflection explains enhanced ASR (~42°S peak in Figure 1a). In the sea ice loss zone (55–70°S), cloud brightening and surface albedo reductions have competing effects on ASR changes (Figure 1b).

When compared to early 21st century observations (Clouds and the Earth's Radiant Energy System-Energy Balanced and Filled (CERES-EBAF)) [*Loeb et al.*, 2009], CESM-CAM5 has excessive ASR at all Southern Ocean latitudes (Figure 1c). When annually averaged, the ensemble mean 21st century Southern Ocean ASR change (+3.7 W m^{-2}) is approximately half the magnitude of the ensemble mean early 21st century Southern Ocean ASR bias (+8.1 W m^{-2}). This relatively large ASR bias raises concern with using CESM-CAM5 as a tool to identify processes controlling Southern Ocean ASR changes. While biases may imprint on changes, we did not find simple relationships between biases and changes.

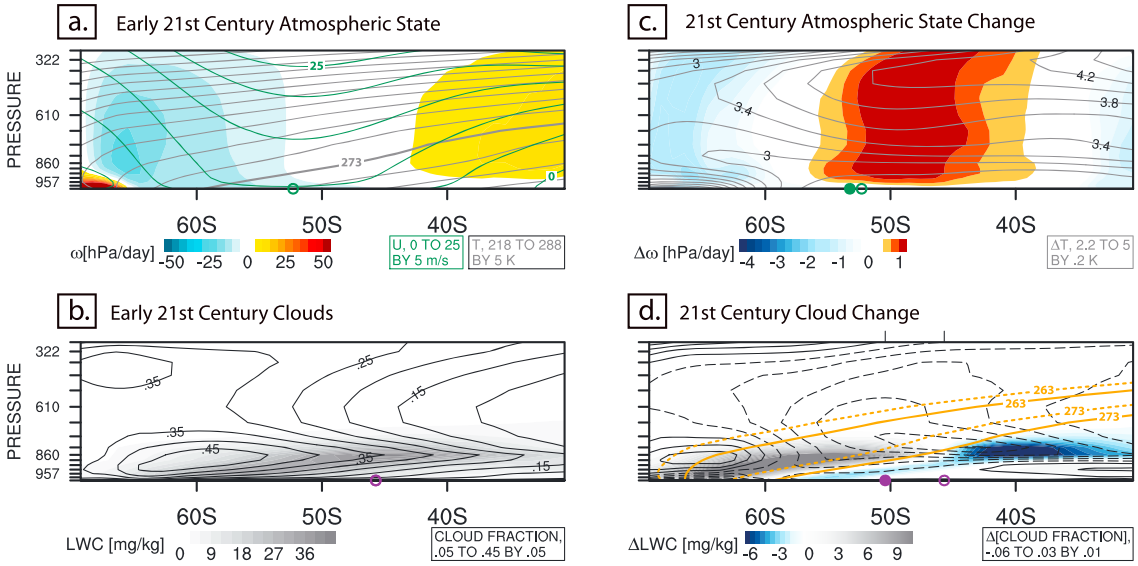

Figure 2. Annual zonal mean RCP8.5 CESM-CAM5 Southern Ocean atmospheric state and clouds: (a) Early 21st century (2006–2025) atmospheric state: westerly wind speed (green lines), subsidence (filled contours), and temperature (grey lines, melting level ($T = 273$ K) thicker); (b) Early 21st century clouds: cloud fraction (grey lines) and cloud liquid water (LWC) content (filled contours); (c) 21st century atmospheric state change (2080–2099 minus 2006–2025): subsidence (filled color contours) and temperature (grey contours); (d) 21st century cloud change: cloud fraction (grey contours, dash negative, solid positive) and cloud LWC (filled contours). Orange lines indicate melting level and $T = 263$ K in the early 21st century (solid) and late 21st century (dotted). Green (purple) circles on *x* axis of Figures 2a and 2c (Figures 2b and 2d) show jet latitude (max(LWP) latitude) for the early 21st century (open circle) and late 21st century (filled circle).

3.2. Processes Controlling 21st Century Cloud Changes in CESM-CAM5

Unlike enhanced ASR due to sea ice loss, the sign of the cloud-induced ASR changes depends on latitude (Figure 1b). Thus, we next examine processes controlling 21st century Southern Ocean cloud changes. We set the stage by first describing the early 21st century mean state (Figures 2a and 2b). Over the Southern Ocean, there is mean subsidence associated with the descending branches of the Hadley circulation and the Ferrel cell (30–50°S, "subsidence regime") and mean ascent in the storm track (50–70°S, "ascent regime") (color contours, Figure 2a). Strong westerly winds from the eddy-driven midlatitude jet peak in the upper troposphere (green contours, Figure 2a). The latitude of the maximum 850 mb westerly wind speed, hereafter the *jet latitude*, occurs at 52°S (circle on *x* axis). The annual mean melting line intersects the surface at 60°S (bold grey contour). In the subsidence regime, subsidence warming balances radiative cooling throughout much of the troposphere. As a result, there is a cumulus-capped boundary layer but the overlying troposphere is cloud free (Figure 2b). In contrast, baroclinic disturbances and frontal lifting occur in the ascent regime and thus, relatively large cloud fractions extend up to ~300 mb.

In both the subsidence and ascent regimes, the radiatively important clouds (i.e., the clouds that most strongly influence rCRE) are the low-level liquid clouds. The latitude of the maximum cloud liquid water path (LWP, vertical sum of liquid water content (LWC)), hereafter the *max(LWP) latitude*, occurs at 46°S (circle on the *x* axis, Figure 2b). The latitude of the maximum cloud fraction (62°S) is farther poleward than the max(LWP) latitude.

Having set the stage, we next present change. Over the 21st century, CESM-CAM5 projects a poleward jet latitude shift from 52°S to 53°S (green circles on *x* axis, Figure 2c). This jet shift is relatively small when compared to other models [*Barnes and Polvani*, 2013], consistent with the CESM-CAM5 jet being located farther poleward than it is in other models [*Kidston and Gerber*, 2010]. Westerly wind speeds increase from 45 to 70°S (not shown), consistent with a pulse-like (intensity) response in CESM-CAM5 as opposed to the wobble (location) response seen in models with a more equatorward eddy-driven jet [*Barnes and Polvani*, 2013].

In addition to a poleward jet shift and increased westerly wind speeds, subsidence increases on the equatorward side of the jet (Figure 2c). Increased subsidence reduces relative humidity and cloud fractions

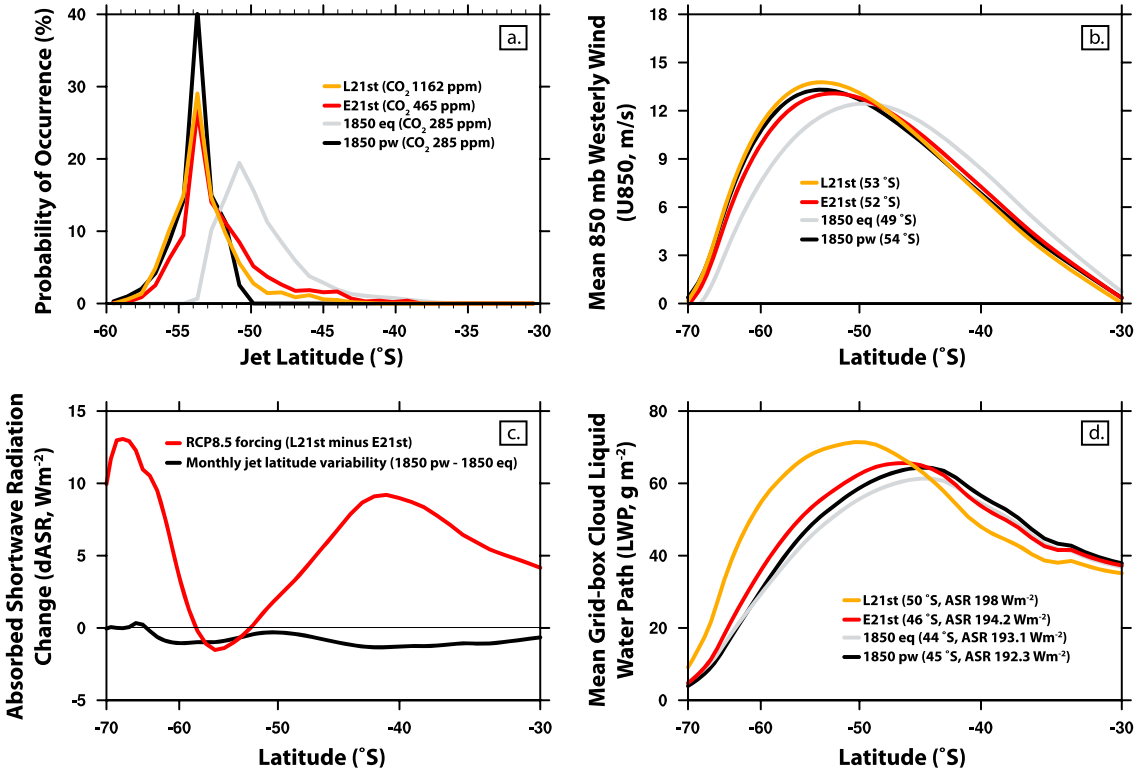

Figure 3. CESM-CAM5 Southern Ocean changes resulting from 21st century RCP8.5 forcing and from natural jet latitude variability: (a) histograms of monthly mean jet latitude, (b) zonal annual mean westerly wind speed at 850 mb (U850), (c) zonal annual mean ASR change resulting from 21st century RCP8.5 forcing (L21st − E21st) and natural poleward jet latitude shifts (1850 pw–1850 eq), (d) zonal annual grid-box mean cloud LWP. Figure 3a indicates equivalent carbon dioxide concentrations. Figure 3b indicates mean jet latitudes. Figure 3d indicates mean max(LWP) latitude and Southern Ocean ASR.

throughout much of the free troposphere (Figure 2d). Similar poleward jet shift-subsidence-cloud fraction relationships have been identified by analyzing variability and ozone forcing in models [*Hall and Visbeck*, 2002; *Grise et al*., 2013] and observations [*Grise et al*., 2013; *Bender et al*., 2011].

Over the 21st century, cloud LWC increases in the ascent regime but decreases in the subsidence regime (Figure 2d). As a result, the max(LWP) latitude shifts poleward from 46°S to 50°S (purple circles on *x* axis of Figure 2d). Although they both shift poleward, the 4° max(LWP) latitude shift is much more pronounced than the 1° jet latitude shift. Important for the climate feedbacks, the max(LWP) latitude shift can explain the trough-peak shape of the cloud-induced ASR changes (Figures 1b and S1d). In contrast, neither the jet latitude shift nor the cloud fraction changes are consistent cloud-induced ASR changes.

Lower tropospheric stability changes and warming are both promising candidates to explain 21st century radiatively important clouds changes. In CESM-CAM5, the cloud LWC changes in Figure 2d are produced by mass flux and detrainment changes in the shallow convection scheme [*Gettelman et al*., 2012], which is strongly influenced by lower tropospheric stability. All else being equal, warming increases the water vapor available to be condensed (Clausius Clapeyron). Above the melting level, warming also promotes cloud liquid increases at the expense of cloud ice decreases.

Although it is tempting to describe the LWC changes in Figure 2d in terms of a max(LWP) latitude shift, it appears that distinct processes occurring within the subsidence and ascent regimes explain these changes. In the subsidence regime, lower tropospheric stability increases, not warming, are consistent with decreased cloud LWC (Figure 2c). Though the location of the subsidence regime changes seasonally, lower tropospheric stability increases and cloud LWC decreases occur in all seasons (not shown). In the ascent regime, both warming and lower tropospheric stability decreases can explain increased cloud LWC. Because ascent regime LWC changes occur above the melting level, warming effects via both Clausius Clapeyron and phase changes could be

important. In the sea ice loss zone (~55–70°S), decreased near-surface stability may also contribute to increased LWC. In this zone, the low-level cloud base rises (Figure 2d) and surface moisture fluxes increase (not shown). While evident in the annual mean, near-surface stability decreases associated with sea ice loss are absent in summer (DJF) (Figure S1c). Thus, warming alone may explain summer LWC increases. More sophisticated diagnostics (beyond the scope here) are needed to disentangle the influence of sea ice loss and warming on cloud LWC changes.

3.3. Greenhouse Gas Forcing Versus Natural Jet Latitude Variability

Intrigued by the surprising disconnect between 21st century jet shifts and radiatively important cloud changes, we next contrast jet, cloud, and ASR changes resulting from 21st century RCP8.5 forcing with those that result from natural jet latitude variability in the 1850 control run. Because monthly mean jet latitude varies, we created equatorward-shifted and poleward-shifted 1850 jet composites in each month before aggregating to evaluate the annual mean influence of natural jet latitude variability on ASR.

We first present jet latitude histograms (Figure 3a) and zonal mean 850 mb westerly winds (Figure 3b). The 5° difference in the mean jet latitude of the equatorward-shifted and poleward-shifted 1850 jet composites (49°S versus 54°S) is much larger than the 1° poleward jet latitude shift over the 21st century (52°S to 53°S).

We next contrast the ASR changes resulting from natural jet latitude variability and 21st century RCP8.5 forcing (Figure 3c). Natural poleward jet latitude shifts result in small (<1 W m^{-2}) near-uniform zonal mean ASR reductions from 30 to 65°S. When averaged over the Southern Ocean, natural poleward jet shifts result in a 0.8 W m^{-2} ASR decrease, while 21st century RCP8.5 forcing results in a much larger 3.8 W m^{-2} ASR increase. Comparing the poleward-shifted 1850 jet composite to the late 21st century, their annual mean jet latitudes are within 1° of each other and their zonal mean 850 hPa winds are similar, yet their annual mean Southern Ocean ASR differs by 5.7 W m^{-2}. The LWP differences in Figure 3d are consistent with the ASR differences in Figure 3c.

4. Discussion

4.1. Radiatively Important Cloud Changes Are Not Consistent With Jet Shifts

Clouds are tracers for the large-scale atmospheric circulation. Thus, it makes sense to hypothesize that large-scale atmospheric circulation changes will affect cloud-climate feedbacks. Though the underlying physical mechanisms are not fully understood, poleward jet/storm track shifts have been identified as a robust circulation response to increased greenhouse gases and the ozone hole in models [*Thompson et al*., 2011; *Yin*, 2005], and are especially prominent in the Southern Hemisphere [*Barnes and Polvani*, 2013]. Indeed, direct connections between poleward jet shifts and clouds are commonly discussed in both observations and models [*Grise et al*., 2013; *Bender et al*., 2011; *Thompson et al*., 2011; *Hwang and Frierson*, 2010; *Hall and Visbeck*, 2002].

Based on existing studies, we were surprised to find that CESM-CAM5 Southern Hemisphere jet shifts exert such a small influence on radiatively important clouds and ASR (Figure 3c). Since radiation is what matters for climate feedbacks, this relatively small influence of jet shifts on radiatively important clouds is important. This small influence is counterintuitive because it goes against the conventional paradigm that midlatitude cloud structures are slaved to the large-scale, baroclinic disturbances; the location of which can be predicted by the jet. Our results show that the jet is not a primary driver of radiatively important cloud processes and, therefore, not a primary driver of radiatively important cloud changes. Radiatively important low-level liquid clouds are influenced by temperature and lower tropospheric stability; both of which can change in the absence of jet shifts.

4.2. CESM-CAM5 Biases and Reproducibility

How do model biases in CESM-CAM5 affect the reliability of these results? A bias that is unlikely to adversely affect CESM-CAM5 results is jet location. Unlike many climate models, which have their jets too far equatorward, the CESM-CAM5 late twentieth century (1979–2005) jet latitude (52°S) is within 1° of reanalysis products (51°S) [*Ceppi et al*., 2012]. Having a realistic jet location is important because the jet response depends on the jet location [*Kidston and Gerber*, 2010]. In contrast, CESM-CAM5 has excessive Antarctic sea ice extent (not shown), and thus,

presented ASR changes associated with Antarctic sea ice loss (Figure 1b) are likely more pronounced than what we might expect to observe. Substantial Southern Ocean cloud and associated radiation biases also exist in CAM5 [*Kay et al.*, 2012], but it is unclear how to simply relate these cloud biases to cloud changes.

While evaluation of cloud-jet-ASR relationships in many models is an important next step, it is beyond the scope of this work. We did, however, assess the robustness of these results using Community Climate System Model version 4 (CCSM4) [*Gent et al.*, 2011] (Figure S2). Aside from its atmospheric physics, CCSM4 is the same model as CESM-CAM5. Jet location, natural jet variability, and 21st century jet shifts are similar in the two models, but CCSM4 suffers from more severe extensive Antarctic sea ice biases, Southern Ocean ASR biases (annual mean bias +13.7 W m^{-2}) and cloud biases [*Kay et al.*, 2012]. Comparison of CESM-CAM5 and CCSM4 suggests that two results are robust. First, sea ice and thermodynamically driven cloud changes, not poleward jet shifts, control 21st century ASR changes. Second, 21st century ASR changes are much larger than the ASR changes resulting from natural jet latitude variability. Interestingly, the influence of natural jet variability on ASR is different in the two models (Figure 3c versus Figure S2c).

5. Conclusions

In CESM-CAM5, sea ice loss and low-level liquid cloud changes resulting from warming and stability changes explain Southern Ocean shortwave climate feedbacks in response to 21st century RCP8.5 forcing. In contrast, natural jet variability and RCP8.5-forced jet shifts have a relatively small influence on shortwave climate feedbacks. Additional process-oriented analyses of models and observations are needed to understand the influence of greenhouse gas forcing, ozone forcing, and jet variability on the sea ice and radiatively important clouds that control Southern Ocean climate feedbacks.

Acknowledgments

Funding was provided by the U.S. NSF through NCAR and the Office of Science (BER), U.S. DOE. We thank L. Polvani, P. Caldwell, A. Solomon, J. Fasullo, M. Zelinka, and two reviewers (K. Grise, anonymous) for their helpful feedbacks, as well as those who developed CESM-CAM5 and CCSM4 and NCAR's Computational and Information Systems Laboratory.

The Editor thanks two anonymous reviewers for their assistance in evaluating this paper.

References

Barnes, E. A., and L. M. Polvani (2013), Response of the midlatitude jets and of their variability to increased greenhouse gases in the CMIP5 models, *J. Clim.*, *26*, 7117–7135, doi:10.1175/JCLI-D-12-00536.1.

Bender, F. A.-M., V. Ramanathan, and G. Tselioudis (2011), Changes in extratropical storm track cloudiness 1983–2008: Observational support for a poleward shift, *Clim. Dyn.*, *38*, 2037–2053, doi:10.1007/s00382-011-1065-6.

Bodas-Salcedo, A., et al. (2013), Origins of the solar radiation biases over the Southern Ocean in CFMIP2 models, *J. Clim.*, doi:10.1175/JCLI-D-13-00169.1, in press.

Ceppi, P., Y.-T. Hwang, D. M. W. Frierson, and D. L. Hartmann (2012), Southern Hemisphere jet latitude biases in CMIP5 models linked to shortwave cloud forcing, *Geophys. Res. Lett.*, *39*, L19708, doi:10.1029/2012GL053115.

Fitzpatrick, M. F., and S. G. Warren (2007), The relative importance of clouds and sea ice for the solar energy budget of the southern ocean, *J. Clim.*, *20*, 941–954, doi:10.1175/JCLI4040.1.

Flanner, M. G., K. M. Shell, M. Barlage, D. K. Perovich, and M. A. Tschudi (2011), Radiative forcing and albedo feedbacks from the Northern Hemisphere cryosphere between 1979 and 2008, *Nat. Geosci.*, *4*, 151–155, doi:10.1038/ngeo1062.

Gent, P. R., et al. (2011), The Community Climate System Model Version 4, *J. Clim.*, *24*, 4973–4991, doi:10.1175/2011JCLI4083.1.

Gettelman, A., J. E. Kay, and K. M. Shell (2012), The evolution of climate sensitivity and climate feedbackss in the Community Atmosphere Model, *J. Clim.*, *25*, 1453–1469, doi:10.1175/JCLI-D-11-00197.1.

Grise, K. M., L. M. Polvani, G. Tselioudis, Y. Wu, and M. D. Zelinka (2013), The ozone hole indirect effect: Cloud-radiative anomalies accompanying the poleward shift of the eddy-driven jet in the Southern Hemisphere, *Geophys. Res. Lett.*, *40*, 3688–3692, doi:10.1002/grl.50675.

Hall, A., and M. Visbeck (2002), Synchronous variability in the southern hemisphere atmosphere, sea ice, and ocean resulting from the annular mode, *J. Clim.*, *15*, 3043–3057.

Haynes, J. M., C. Jakob, W. B. Rossow, G. Tselioudis, and J. Brown (2011), Major characteristics of Southern Ocean cloud regimes and their effects on the energy budget, *J. Clim.*, *24*, 5061–5080, doi:10.1175/2011JCLI4052.1.

Hurrell, J., et al. (2013), The Community Earth System Model: A framework for collaborative research, *Bull. Am. Meteorol. Soc.*, doi:10.1175/BAMS-D-12-00121.1.

Hwang, Y.-T., and D. M. W. Frierson (2010), Increasing atmospheric poleward energy transport with global warming, *Geophys. Res. Lett.*, *37*, L24807, doi:10.1029/2010GL045440.

Hwang, Y.-T., and D. M. W. Frierson (2013), A link between the double intertropical convergence zone problem and cloud biases over the Southern Ocean, *Proc. Natl. Acad. Sci.*, doi:10.1073/pnas.1213302110.

Kay, J. E., et al. (2012), Exposing global cloud biases in the Community Atmosphere Model (CAM) using satellite observations and their corresponding instrument simulators, *J. Clim.*, *25*, 5190–5207, doi:10.1175/JCLI-D-11-00469.1.

Kidston, J., and E. P. Gerber (2010), Intermodel variability of the poleward shift of the austral jet stream in the CMIP3 integrations linked to biases in 20th century climatology, *Geophys. Res. Lett.*, *37*, L09708, doi:10.1029/2010GL042873.

Lamarque, J.-F., et al. (2011), Global and regional evolution of short-lived radiatively active gases and aerosols in the Representative Concentration Pathways, *Clim. Change*, doi:10.1007/s10584-011-0155-0.

Lefebvre, W., and H. Goosse (2008), Analysis of the projected regional sea-ice changes in the Southern Ocean during the twenty-first century, *Clim. Dyn.*, *30*, 59–76, doi:10.1007/s00382-007-0273-6.

Loeb, N. G., et al. (2009), Toward optimal closure of the Earth's top-of-atmosphere radiation budget, *J. Clim.*, *22*, 748–766, doi:10.1175/2008JCLI2637.1.

Meinshausen, M., et al. (2011), The RCP greenhouse gas concentrations and their extension from 1765 to 2300, *Clim. Change*, (Special Issue), doi:10.1007/s10584-011-0156-z.

Thompson, D. W. J., S. Solomon, P. J. Kushner, M. H. England, K. M. Grise, and D. J. Karoly (2011), Signatures of the Antarctic ozone hole in Southern Hemisphere surface climate change, *Nat. Geosci.*, *4*, 741–749, doi:10.1038/ngeo1296.

Trenberth, K. E., and J. T. Fasullo (2010), Simulation of present-day and twenty-first-century energy budgets of the Southern Oceans, *J. Clim.*, *23*, 440–454, doi:10.1175/2009JCLI3152.1.

Tsushima, Y., S. Emori, T. Ogura, M. Kimoto, M. J. Webb, K. D. Williams, M. A. Ringer, B. J. Soden, B. Li, and N. Andronova (2006), Importance of the mixed-phase cloud distribution in the control climate for assessing the response of clouds to carbon dioxide increase: A multi-model study, *Clim. Dyn.*, *27*, 113–126, doi:10.1007/s00382-006-0127-7.

Vial, J., J.-L. Dufresne, and S. Bony (2013), On the interpretation of inter-model spread in CMIP5 climate sensitivity estimates, *Clim. Dyn.*, *1–24*, doi:10.1007/s00382-013-1725-9.

Williams, K. D., et al. (2013), The Transpose-AMIP II experiment and its application to the understanding of Southern Ocean cloud biases in climate models, *J. Clim.*, *26*, 3258–3274, doi:10.1175/JCLI-D-12-00429.1.

Yin, J. H. (2005), A consistent poleward shift of the storm tracks in simulations of 21st century climate, *Geophys. Res. Lett.*, *32*, L18701, doi:10.1029/2005GL023684.

Zelinka, M. D., S. A. Klein, K. E. Taylor, T. Andrews, M. J. Webb, J. M. Gregory, and P. M. Forster (2013), Contributions of different cloud types to feedbacks and rapid adjustments in CMIP5, *J. Clim.*, *26*, 5007–5027, doi:10.1175/JCLI-D-12-00555.1.